A&A 398, 141–151 (2003)
DOI: 10.1051/0004-6361:20021615

Astronomy & Astrophysics

Vertical distribution of Galactic disk stars⋆

I. Kinematics and metallicity

C. Soubiran[1], O. Bienaymé[2], and A. Siebert[2]

[1] Observatoire Aquitain des Sciences de l'Univers, UMR 5804, 2 rue de l'Observatoire, 33270 Floirac, France
[2] Observatoire astronomique de Strasbourg, UMR 7550, Université Louis Pasteur, Strasbourg, France

Received 3 July 2002 / Accepted 22 October 2002

Abstract. Nearly 400 Tycho-2 stars have been observed in a 720 square degree field in the direction of the North Galactic Pole with the high resolution echelle spectrograph ELODIE. Absolute magnitudes, effective temperatures, gravities and metallicities have been estimated, as well as distances and 3D velocities. Most of these stars are clump giants and span typical distances from 200 pc to 800 pc to the galactic mid-plane. This new sample, free of any kinematical and metallicity bias, is used to investigate the vertical distribution of disk stars. The old thin disk and thick disk populations are deconvolved from the velocity-metallicity distribution of the sample and their parameters are determined. The thick disk is found to have a moderate rotational lag of $-51 \pm 5\,\mathrm{km\,s^{-1}}$ with respect to the Sun with velocity ellipsoid $(\sigma_U, \sigma_V, \sigma_W) = (63 \pm 6, 39 \pm 4, 39 \pm 4)\,\mathrm{km\,s^{-1}}$, mean metallicity of [Fe/H] $= -0.48 \pm 0.05$ and a high local normalization of $15 \pm 7\%$. Combining this NGP sample with a local sample of giant stars from the Hipparcos catalogue, the orientation of the velocity ellipsoid is investigated as a function of distance to the plane and metallicity. We find no vertex deviation for old stars, consistent with an axisymmetric Galaxy. Paper II is devoted to the dynamical analysis of the sample, puting new constraints on the vertical force perpendicular to the galactic plane and on the total mass density in the galactic plane.

Key words. stars: kinematics – stars: abundances – Galaxy: disk – Galaxy: kinematics and dynamics – Galaxy: structure – Galaxy: solar neighbourhood

1. Introduction

The primary purpose of the observations described in this paper is to determine the potential from 300 pc to 1 kpc from the galactic plane using an homogeneous and complete sample of red clump giants. The measure of the potential close to the galactic plane has been recently improved thanks to the Hipparcos observations leading to an unbiased estimate of the local mass density $0.076 \pm 0.015\,M_\odot\,\mathrm{pc}^{-3}$ (based on A and F stars, Crézé et al. 1998a,b, see also Pham 1998 and Holmberg & Flynn 2000) constraining the potential shape up to 125 pc from the galactic plane. This result is consistent with previous and independent determinations based on distant F dwarfs and K giants at 0.5–1 kpc (Kuijken & Gilmore 1989). A direct implication of these results is that our galactic dark matter component cannot be strongly flattened and has a more or less spheroidal shape. In order to draw with an improved accuracy the potential at various heights from the galactic plane and confirm or not this property, new kinematical data appeared to be necessary.

For this task we have chosen to observe red clump giants which are well suited for galactic studies. The first and evident interest in studying giants is their intrinsic brightness, ($m_V \simeq 9.3$ at 500 pc) that allows to obtain high-resolution spectroscopy on distant stars. Moreover clump giants have a high density in the solar neighbourhood as compared to other intrinsically bright stars, they dominate in the magnitude interval $9 \leq m_v \leq 10.5$ and colour interval $0.9 \leq B - V \leq 1.1$. Thanks to their strong-lined spectra, K stars are well adapted to the measure of accurate radial velocities and atmospheric parameters: effective temperature $T_{\rm eff}$, logarithm of gravity $\log g$ and metallicity measured by the iron abundance [Fe/H]. In practice, atmospheric parameters were deduced from low S/N (∼20) ELODIE spectra using the automated method of parametrisation TGMET, based on a criterion of minimum distance to an empirical library of reference spectra (Katz et al. 1998; Soubiran et al. 1998). The same principle is used to estimate the absolute magnitude of the target stars, leading to distances with an accuracy better than 20%, unprecedented for K giants out of the 250 pc Hipparcos sphere.

Send offprint requests to: C. Soubiran,
e-mail: Caroline.Soubiran@observ.u-bordeaux.fr

⋆ Based on observations made at the Observatoire de Haute Provence (France). Data are only available in electronic form at the CDS via anonymous ftp to cdsarc.u-strasbg.fr (130.79.125.5) or via
http://cdsweb.u-strasbg.fr/cgi-bin/qcat?J/A+A/398/141

This new sample has been used to determine the vertical force K_z and the disk surface mass density as described in Paper II. These data have also provided an opportunity to probe the transition between the thin and thick disks and to investigate their properties. If the existence of a thick disk in our Galaxy is well established, its formation and connexion to the thin disk are still matters of debate. Several models of formation, "top down" or "bottom-up" are proposed which predict peculiar features for the spatial, chemical, kinematical and age distributions of the thick disk, including mean behaviour and dispersions, gradients, continuity-discontinuity with other populations. Such predictions are described for instance in Majewski (1993). Therefore, a detailed knowledge of properties of the thick disk is necessary to favour one of the proposed models of formation. Previous studies of the thick disk properties are numerous but most of them suffer from serious limitations: local samples of selected stars are biased in favour of metal-poor or high velocity stars, samples of tracers (clusters, RR Lyrae...) are small and not necessary representative of the whole thick disk population, while in situ surveys suffer from lower precision due to the lack of astrometric and spectroscopic observations for faint stars. As a consequence, the parameters of the thick disk are not precisely established. Its current status is given in Norris (1999). There is still a controversy between the partisans of a flat and dense thick disk, with typical scale height of 800 pc and local relative density of 6–7% (Reylé & Robin 2001), and the partisans of a thick disk with a higher scale height, typically 1300 pc and a lower local relative density, of the order of 2% (Reid & Majewski 1993; Chen 1997). Velocity ellipsoid, asymmetric drift and mean metallicity are the other parameters which characterize the thick disk. Velocity dispersions are generally found to span typical values between 30 and 50 km s^{-1}, sometimes up to 80 km s^{-1} in the radial direction (Ratnatunga & Freeman 1989). The asymmetric drift ranges between −20 and −80 km s^{-1} and the mean metallicity from −0.50 to −0.80 dex. The view of the thick disk has been complicated by the study of Morrison et al. (1990) who brought to the fore low-metallicity stars ($-1.6 <$ [Fe/H] < -1.0) with disk-like kinematics. Chiba & Beers (2000) estimate that 30% of the stars with $-1.6 <$ [Fe/H] < -1.0 belong to the thick disk population. It remains unclear whether this population is separate from the thick disk or its metal-weak tail. Very recently, Gilmore et al. (2002) claimed to have observed the relics of a shredded satellite forming a thick disk rotating at 100 km s^{-1} at several kpc from the plane. A better understanding of the thick disk population(s) can be achieved from accurate distances, 3D velocities and metallicities for large samples of stars, with no kinematical or chemical selection, far from the plane where the relative density of the thick disk is high. Thanks to our new complete and large sample of K giants at a mean height of 400 pc above the plane, the old thin disk and thick disk populations were investigated with an unprecedented accuracy on distances, velocities and metallicities. Combining metallicities and velocities, we were able to deconvolve the thin disk and thick disk distributions providing new estimates of their parameters.

The change of the velocity ellipsoid with respect to height above the plane and metallicity has also been investigated. If the stationarity and axisymmetry of the Galaxy is generally considered as a good approximation, large scale deviations produced by warps, bars, or triaxiality of the halo, are also often mentioned. The orientation of the velocity ellipsoid is an indicator of such deviations. In the case of axisymmetry and stationarity, the velocity ellipsoid of the oldest stars is supposed to point towards the Galactic Center. This is the case in our NGP sample.

The analysis of the sample has been carried out with different tools. For the validation of our methods and for the interpretation of the stellar content of our dataset, we have used simulations of the Besançon model of stellar population synthesis of the Galaxy (Robin & Crézé 1986; Robin et al. 2002). The deconvolution of the thin disk and thick disk distributions has been performed in the 4D velocity-metallicity space using a maximum likelihood algorithm assuming Gaussian components.

In Sect. 2 we describe the selection of the sample to optimize the number of clump giants. Section 3 is devoted to the determination of stellar parameters: radial velocities, atmospheric parameters ($T_{\rm eff}$, log g, [Fe/H]), absolute magnitudes M_v, distances, 3D velocities with respect to the Sun. In Sect. 4, observed vertical gradients are compared to simulations of the Besançon model, and the deconvolution of two components is described. Section 5 deals with the vertex deviation. Our conclusions are summarized in Sect. 6.

2. Selection of the sample

The bulk of our sample consists of stars selected out of the Tycho-2 catalogue (Høg et al. 2000). This catalogue provides $V_{\rm T}$ magnitudes, $B_{\rm T} - V_{\rm T}$ colours, accurate proper motions and related errors. Tycho-2 photometry can be transformed into Johnson photometry applying the transformation given in ESA (1997, Chap. 1)

$$V = V_{\rm T} - 0.090\,(B_{\rm T} - V_{\rm T})$$
$$B - V = 0.850\,(B_{\rm T} - V_{\rm T}). \quad (1)$$

A selection in $B - V$ colour has been applied to increase the number of red clump stars with respect to dwarfs, subgiants, RGB and AGB stars. We have looked at several studies, based on Hipparcos data, which use and discuss the properties of the position of the red clump in the HR diagram, used for instance as distance indicator for the galactic center (Paczynski 1998) or nearby galaxies (Girardi & Salaris 2001). According to these studies, we have chosen the colour interval $0.9 < B - V < 1.1$ that optimizes the detection of red clump stars. The lower $B-V$ limit at 0.9 rejects the brightest main sequence stars ($M_{\rm V} < 5$), some subgiants and also most giants of the blue horizontal branch (the "clump stars" with the lowest metallicities). The upper $B - V$ limit at 1.1 rejects most of RGB and AGB stars. We have set the limiting magnitude at $V = 10.5$ to limit the exposure time of the spectroscopic observations, also because dwarfs begin to be dominant at fainter magnitude. Observing conditions have finally lowered the limiting magnitude of the sample.

In order to have a regular distribution of stars versus distance to the galactic plane, the survey has been carried out on

two circular fields towards the NGP. The two observed fields have different size and limiting apparent magnitude (Table 1). The first one is shifted by 10 degrees from the NGP to avoid the region of the Coma–Berenices open cluster ($\ell = 221°$, $b = +84°$). A circular region of 4.5° radius around the center of the cluster has been removed from the second field centred on the NGP. As the two fields overlap, the common region is defined as belonging to the deepest field. Some stars were excluded a priori from the observations: i) stars identified as dwarfs thanks to their accurate Hipparcos parallaxe, ii) stars identified as variable or multiple system.

A total of 387 stars have been observed with the Elodie echelle spectrograph at OHP, 8 of them have been observed twice. According to individual errors quoted in the Tycho-2 catalogue, the sample has a mean error of 1.3 mas yr^{-1} on proper motions, corresponding to an error of 3.25 km s^{-1} on tangential velocities at 500 pc. The characteristics of the two fields are summarized in Table 1.

3. Stellar parameters

3.1. Spectroscopic observations, radial velocities

The observations were carried out with the echelle spectrograph Elodie on the 1.93 m-telescope at the Observatoire de Haute Provence. The performances of this instrument are described in Baranne et al. (1996). A total of 22 nights was attributed to this program in March-April 2000 and April-May 2001. The exposure time on individual targets ranges from 90 s to 35 min, with a mean value of 9 min and a total of 61 hours. The resulting spectra cover the full range 390–680 nm at a resolving power of 42 000. Spectrum extraction, wavelength calibration and measurement of radial velocities have been performed at the telescope with the on-line data reduction software. The radial velocity accuracy is better than 1 km s^{-1} for the considered stars (K stars). Our sample spans radial velocities from −92 to 85 km s^{-1} with a mean value of −13.5 km s^{-1}. The mean S/N of the spectra at 550 nm is 23.

3.2. Atmospheric parameters (T_{eff}, log g, [Fe/H]) and absolute magnitudes M_v

3.2.1. TGMET and its library of reference spectra

Atmospheric parameters and absolute magnitudes were obtained with the TGMET software (Katz et al. 1998). TGMET is a minimum distance method (reduced χ^2 minimisation) which measures similarities between spectra in a quantitative way and finds for a given target spectrum the most closely matching template spectra in a library. The TGMET library was built from the ELODIE database described in Prugniel & Soubiran (2001), selecting high S/N spectra of reference stars having well known atmospheric parameters from published detailed analyses listed in the Catalogue of [Fe/H] determinations (Cayrel de Strobel et al. 2001). The selection of reference stars was extended to stars with published $T_{\rm eff}$ from the lists of Blackwell & Lynas-Gray (1998); di Benedetto (1998); Alonso et al. (1996a, 1999a) and to stars with available $V - K$ colour index in the catalogue of Morel & Magnenat (1978), calibrated into $T_{\rm eff}$ using the formulae of Alonso et al. (1996b, 1999b). Multiple determinations of atmospheric parameters for the same reference star were averaged, giving more weight to the most recent analyses.

Thanks to TGMET, absolute magnitudes M_v were estimated simultaneously with the atmospheric parameters, based on the fact that stars having similar spectra have similar absolute magnitudes. Therefore, the TGMET reference library was completed with Hipparcos stars having parallaxes with a relative error lower than 30%. Their absolute magnitudes M_v were derived from the Tycho-2 $V_{\rm T}$ apparent magnitude, transformed into V Johnson band, and these stars were used as reference stars for M_v. Finally the TGMET library which was used in this study included 1112 spectra of FGK stars, 598 with available $T_{\rm eff}$ from the literature, 558 with available log g, 577 with available [Fe/H], 1079 with available M_v determined from Hipparcos (884 from a parallax with a relative error lower than 10%). The parameters ($T_{\rm eff}$, log g, [Fe/H], M_v) of a target star processed by TGMET are given by the weighted mean of the parameters of the best matching reference spectra.

3.2.2. TGMET external accuracy

The external accuracy of TGMET depends on the quality of the reference system defined by the library of spectra. Ideally the reference library should be a perfect grid, paving regularly the parameter space. In practice, an observed library does not describe all parts of the parameter space with the same sampling. For instance, very metal-poor stars or cool dwarfs are less represented in the library and results of lower quality are expected for this class of stars. Moreover, the reference spectra being parametrized from the literature (and Hipparcos), some errors affect their parameters (typical errors quoted in detailed spectral analyses of the literature range from 50 K to 150 K for $T_{\rm eff}$, 0.1 to 0.3 for log g, and 0.05 to 0.1 for [Fe/H]).

The quality of the library was assessed, and simultaneously the global accuracy of the TGMET atmospheric parameters and absolute magnitudes was estimated. We have tested the ability of TGMET to recover the parameters of stars considered as highly reliable reference stars. For this task we have selected in the library only stars with the smallest error bars on their external parameters, having several determinations of atmospheric parameters in agreement in the literature and a relative parallax error lower than 10% in Hipparcos. For each star of this subset, the corresponding spectrum was removed from the library, its TGMET parameters were estimated with respect to the rest of the library, and compared to the literature and Hipparcos ones, as shown in Fig. 1 for [Fe/H] and M_v. Differences between TGMET and literature parameters have a standard deviation of 0.16 in [Fe/H], and 0.36 in M_v. The standard deviation in M_v is lower for dwarfs than for giants: 0.25 for dwarfs ($M_v > 4$), 0.37 for subgiants ($3 < M_v \leq 4$), 0.32 for clump giants ($0.5 < M_v < 1$), 0.47 for the other giants. Good results for clump giants are explained by the number of reference spectra in the library for this type of stars, with accurate Hipparcos parallaxes.

Table 1. Main characteritics of the two observed fields, l_c and b_c are the galactic coordinate of the center of the fields.

	l_c (deg)	b_c (deg)	limiting magnitude in V_J mag	interval of completeness in V_J mag	number of stars observed	Surface square deg.
Field 1	35.46	80.	10.48	7.2–10.1	246	309.4
Field 2	0.	90.	9.57	7.2–9.2	141	410.1*

* this surface is corrected for the overlap region and for the presence of the Coma Berenices open cluster.

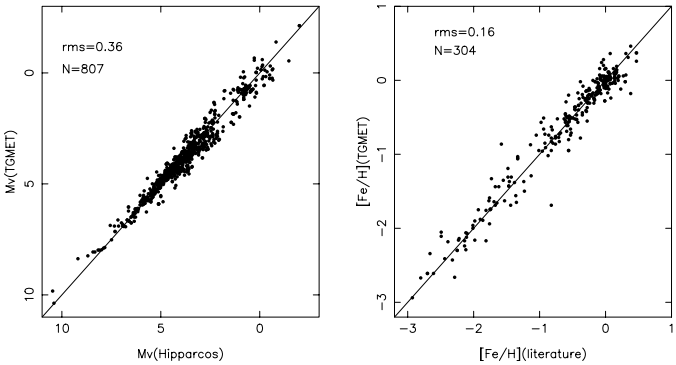

Fig. 1. Comparison of literature metallicities and Hipparcos absolute magnitudes to their TGMET counterparts for a subset of high quality reference stars.

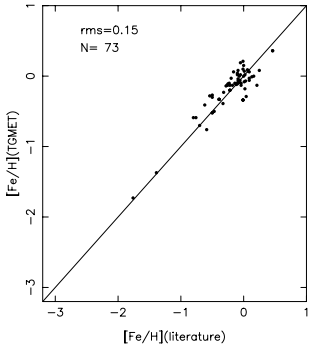

Fig. 2. Comparison of literature and TGMET metallicities for the 73 reference stars which were effectively used to determine the metallicity of the target stars.

In practice only a fraction of the library was useful for TGMET to determine the parameters of the NGP targets: a subset of 117 reference spectra was selected on the basis of their similarity with the targets. These stars have parallax errors ranging from 0.45 to 1.7 mas, with a median of 0.8 mas. The median relative error on parallax of 3.45% for this subset ensures the high quality of our reference system for M_v. Several (16) stars with a relative error greater than 10% correspond to metal poor giants which have to be kept in the library to represent the low metallicity population. The iron abundance of the target stars was determined in practice from 73 reference stars. Their literature and TGMET metallicities are compared in Fig. 2. On average the TGMET metallicities are overestimated by 0.06 dex with an rms of 0.15.

Unfortunatly the absolute magnitudes from Hipparcos parallaxes are affected by the Lutz-Kelker bias, especially among giants. This causes an additional external error which must be taken into account. In Paper II, the Lutz-Kelker bias is estimated for a local sample of clump giants. It is shown that on average their absolute magnitudes have to be corrected by −0.09 mag with an rms of 0.13 mag. We have not attempted to correct individual absolute magnitudes of the reference stars because the Lutz-Kelker bias is estimated from the luminosity function of the parent population which is unknown for most giants of the library, except for the clump ones. Combining the different sources of external errors, we estimate the TGMET absolute magnitudes of clump giants to be affected by a mean error of 0.35 mag, corresponding to an error in distance of 17%, with a systematic overestimation of distances by 4%.

3.2.3. TGMET internal precision

We have investigated the internal precision of TGMET by comparing the parameters obtained on target stars in the case of double observations. The TGMET parameters of the 8 target stars observed twice are given in Table 2. Both solutions show a very good agreement. The results are however of lower quality for T2012-00935, because one of the exposures has the lowest S/N of our observations ($S/N = 5$), at the limit of the possibilities of TGMET, and for T2010-01190 because its spectrum shows an enlarged profile ($FWHM = 15.6\,\mathrm{km\,s^{-1}}$) probably indicating a spectroscopic binary (enlarged profiles with $FWHM > 14\ \mathrm{km\,s^{-1}}$ were only observed for 6 target stars, 2 double lined spectroscopic binaries were detected). Excluding these 2 non-representative cases, we compute rms differences of 0.02 dex in metallicity and 0.075 in absolute magnitude, giving an estimate of the precision of the TGMET method.

3.2.4. The ([Fe/H], M_v) distribution of the NGP sample

The parameters obtained with TGMET for the NGP targets range from 4322 K to 5698 K in $T_{\rm eff}$, from 1.02 to 4.70 in log g, from −1.49 to +0.38 in [Fe/H], from −0.621 to 7.490 in M_v. The most important parameters for this study are the metallicities and absolute magnitudes which lead to individual distances. Figure 3 represents the NGP sample in the plane ([Fe/H], M_v). Some comments have to be done about this plot:

- the sample spans the full range of luminosities, from dwarfs to bright giants;
- the clump is clearly identified as an overdensity around $M_v = 0.81$;
- the selection of giants was efficient: dwarfs or subgiants ($M_v > 3$) represent only 6% of the sample;

Table 2. Comparison of the parameters obtained in the case of double observations. The heliocentric radial velocity V_r was obtained with the on-line cross-correlation software, together with the *FWHM* which measures the true resolution of the spectrum. The atmospheric parameters ($T_{\rm eff}$, $\log g$, [Fe/H]) and absolute magnitudes M_v have been obtained with the TGMET software.

Tycho Id	S/N at 550 nm	V_r km s^{-1}	*FWHM* km s^{-1}	$T_{\rm eff}$ K	$\log g$	[Fe/H]	M_v
T1461-00774	15.8	16.55	11.2	4924	2.74	−0.23	0.756
T1461-00774	15.8	16.50	11.2	4929	2.75	−0.20	0.598
T1462-00831	11.9	1.26	10.7	4807	3.26	0.05	2.077
T1462-00831	21.8	0.89	11.0	4807	3.26	0.05	2.078
T1987-00205	17.5	−27.53	11.3	4776	2.59	−0.20	0.805
T1987-00205	20.4	−27.56	11.2	4765	2.50	−0.19	0.781
T2007-01215	10.5	0.24	12.6	4974	2.82	−0.43	0.647
T2007-01215	23.3	0.09	12.5	4888	2.57	−0.48	0.689
T2010-01190	11.5	−0.02	15.6	4722	2.62	−0.04	0.678
T2010-01190	38.0	−0.08	15.6	4895	3.14	0.15	1.807
T2012-00935	5.0	5.45	11.4	5273	3.56	0.03	3.087
T2012-00935	40.3	5.22	11.1	4918	3.03	−0.07	2.136
T2527-01831	30.4	−28.72	11.3	4801	2.52	−0.02	0.969
T2527-01831	17.5	−28.82	11.3	4804	2.51	−0.03	0.953
T2532-00687	21.3	−66.09	10.9	4711	2.53	−0.53	1.329
T2532-00687	7.9	−66.99	11.0	4709	2.46	−0.54	1.202

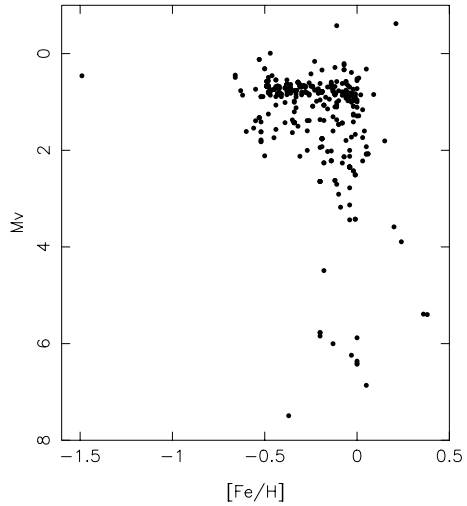

Fig. 3. Metallicity and absolute magnitude distribution of the NGP sample (387 stars).

– there is no dependency of the absolute magnitude of clump giants on [Fe/H];
– there is a cut in the metallicity distribution at [Fe/H] = −0.65 with only one metal-poor star at [Fe/H] = −1.49.

We have checked if the lack of stars with [Fe/H] < −0.65 could be due to the distribution of the TGMET reference stars in the parameter space. According to Fig. 2, several reference stars in the range −1.00 < [Fe/H] < −0.65 exhibit similarities with the targets, but the nearest neighbours are more metal-rich. Several clump giants with lower metallicity exist in the library (HD 166161, HD 175305, HD 044007 for instance) but they have not been selected by TGMET to present similarities with the targets. We conclude that TGMET and its library cannot explain by their own the complete absence of target stars in this metallicity range, even if an overestimation of [Fe/H] by 0.06 was established (Sect. 3.2.2).

Basic data from Tycho2 and TGMET parameters of the 387 NGP targets are given in a table only available in electronic form at the CDS via anonymous ftp to `cdsarc.u-strasbg.fr` (130.79.125.5) or via `http://cdsweb.u-strasbg.fr/cgi-bin/qcat?J/A+A/398/141`

3.3. Distances and spatial velocities

Distances have been computed for all the target stars from the TGMET M_v and Tycho-2 V_T magnitude transformed into Johnson V by relation 1. No correction of interstellar absorption was applied since it is supposed to be very low in the NGP direction. Proper motions, distances and radial velocities have been combined through the equations of Johnson & Soderblom (1987) to compute the 3 velocity components (U, V, W) with respect to the Sun (the U axis points towards the Galactic Center). Figure 4 shows the metallicity and velocity distributions of the whole sample in different combinations. For a sake of clarity, we have excluded from these plots 2 stars with extreme parameters which may belong to the halo: T2004-00702 ([Fe/H] = −1.49, z = 755 pc, U = −133.4 km s^{-1}, V = −145.1 km s^{-1}, W = −54.6 km s^{-1}) and T2524-01735 ([Fe/H] = −0.38, z = 475 pc, U = 40.8 km s^{-1}, V = −280.0 km s^{-1}, W = −37.8 km s^{-1}). From these plots, it can be seen that stars with high radial motion (U < −100 km s^{-1}) or slow rotation (V < −80 km s^{-1}) exist at all metallicities. The velocity dispersions are higher at low metallicities, especially for W. Here we recall that our W velocities are of an unprecedented accuracy for a survey at this mean distance as the contribution of the ELODIE accurate radial velocity to W is higher than 94% in the considered direction.

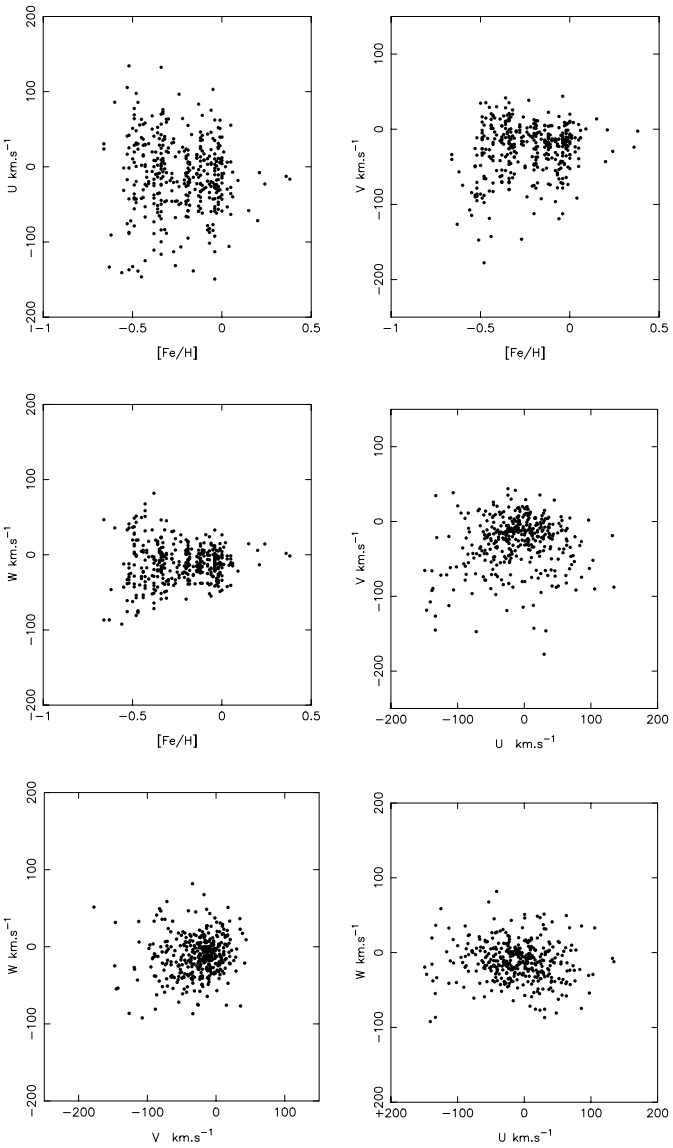

Fig. 4. Distributions of the NGP sample (387 stars) in metallicity and 3D velocities with respect to the Sun.

4. Distances, abundances and kinematics: Stellar components

4.1. Expected relative densities

The median distance of the sample to the galactic plane is 400 pc. We expect to find at this distance a mixture of disk components, mainly the old thin disk and the thick disk. For instance, adopting exponential laws to modelise their vertical density, with a scale height of 300 pc for the older thin disk, 800 pc for the thick disk with a local density of 6.2% (Reylé & Robin 2001), proportions of 9, 13, 18 and 25% of thick disk stars are expected at mean distances of 200, 400, 600 and 800 pc respectively. For a scale height of 1400 pc and a local density of 2% (Reid & Majewski 1993) the proportions of thick disk stars fall to 3, 5, 8 and 13%. With a local relative density well below 1%, the halo population is expected to be marginally represented in the NGP sample. The aim of this section is to identify disk components in the NGP sample, investigate their behaviour up to 800 pc from the plane and determine their mean parameters.

4.2. Comparison with the Besançon model

The NGP sample was compared with several samples of pseudo-stars simulated with the most recent version of the Besançon model of population synthesis (Robin et al. 2002). This model is based on a semi-empirical approach, involving physical constraints and current knowledge of the formation and evolution of the Galaxy. For observing conditions given as inputs (direction and size of the fields, cuts in apparent magnitude and colour, observational errors on apparent magnitudes, proper motions and radial velocities), the model returns a list of pseudo-stars with their fundamental properties (distance, absolute magnitude, age, 3D velocity, metallicity) and the corresponding observables affected by errors. The fundamental properties coming from theoretical distributions, we had to degrade metallicities and absolute magnitudes with the typical errors of the NGP sample to mimic the real data. Metallicities were degraded with a Gaussian error of 0.16 dex and absolute magnitudes with an error varying from 0.25 for dwarfs to 0.35 for clump giants and 0.47 for other giants (see Sect. 3.2.1). Then distances and space velocities were re-computed from degraded absolute magnitudes combined to simulated apparent magnitudes, proper motions and radial velocities.

The Besançon model involves 7 thin disk components with mean ages from 0.15 to 10 Gyr, a thick disk component, a halo and a bulge. We have chosen to test our data against 2 different models: one involving a metal-poor, kinematically hot thick disk (hereafter model 1) and another one less metal deficient and kinematically colder (hereafter model 2). The corresponding parameters used as inputs for the thin disk and the thick disk in both models are given in Table 3. In both cases, the scale height of the thick disk is 800 pc and its relative density in the solar neighbourhood is 6.2%. The asymetric drift of the different components with respect to the Sun ($V_{\rm lag}$) is based on $V_{\rm LSR} = 220\,{\rm km\,s^{-1}}$ and $V_\odot = 6\,{\rm km\,s^{-1}}$. For each model, 3 simulations with our observational conditions have been performed. We have obtained 422, 454, 433 pseudo-stars with model 1 and 395, 434, 422 pseudo-stars with model 2. These numbers have to be compared with the 387 stars of the NGP sample. According to the fact that the NGP sample is not complete down the limiting magnitude, and that several dwarfs and double stars were eliminated a priori, the model counts agree very well with the observations.

We compare in Fig. 5 the vertical gradients of [Fe/H], $V, \sigma_U, \sigma_V, \sigma_W$ which have been obtained by a simple statistic in several bins of distances in the NGP sample, and in the simulated ones which were merged to improve the statistics. In general, the data show a better agreement with model 2 than with model 1. But the error bars on the observed and simulated data are such that it is not possible to favour one of the 2 models from only these vertical gardients. In particular, the V dispersion in the NGP sample is much lower than in both models.

Table 3. Inputs for the old thin disk and thick disk in the Besançon model.

	[Fe/H]	$\sigma_{[Fe/H]}$	V_{lag} km s^{-1}	σ_U km s^{-1}	σ_V km s^{-1}	σ_W km s^{-1}
thin disk 5 Gyr	−0.07	0.18	−17	37	24	15
thin disk 7 Gyr	−0.14	0.17	−21	43	28	18
thin disk 10 Gyr	−0.37	0.20	−21	43	28	18
thick disk model 1	−0.70	0.30	−86	80	60	55
thick disk model 2	−0.48	0.30	−56	60	45	40

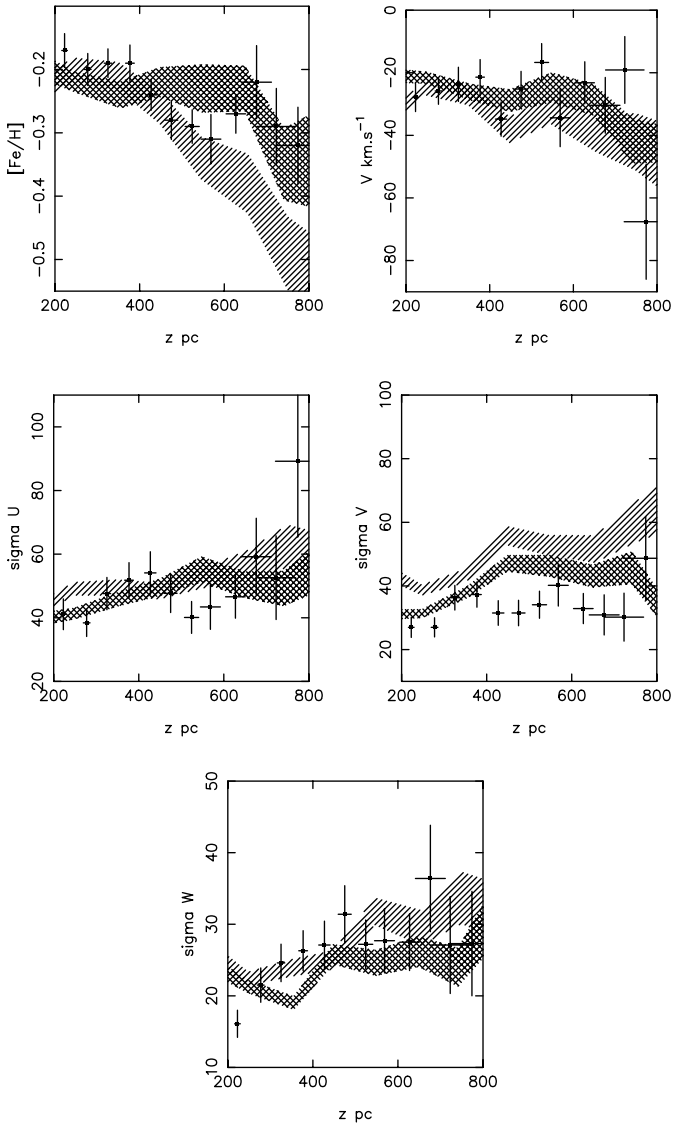

Fig. 5. Vertical gradients of [Fe/H], V, σ_U, σ_V, σ_W with standard error bars. Dots: the NGP sample, hatched area: model 1, double hatched: model 2.

4.3. Deconvolution into Gaussian components

4.3.1. Stochastic estimation maximisation

In an attempt to identify more precisely the contribution of the thin disk and thick disk in the NGP sample, we have performed the deconvolution of these 2 components. We have used the SEM algorithm (Celeux & Diebolt 1986), a noninformative method which solves iteratively the maximum likelihood equations, with a stochastic step, in the case of multivariate mixture of Gaussian distributions. This method has been previously used to deconvolve the thin and thick disk populations from velocity distributions (Soubiran 1993; Ojha et al. 1996). The algorithm is started with an initial position thrown at random, assuming that the sample is a mixture of 2 or 3 discrete components. Each deconvolution is repeated 150 times. Most of the time the algorithm converges the 150 times to the same solution. In case of multiple solutions, the most frequent one is adopted. The combinations of variables ([Fe/H], U, V, W) and (U, V, W) were used. Two bins of distance were considered (200–400 pc and 400–800 pc) to take into account the change of relative densities of the components at various distances to the plane.

4.3.2. Testing SEM on simulated data

Provided that the simulated data represents a mixture of identified components, we have tested the ability of SEM to recover their undelying metallicity and velocity distributions. The SEM outputs are the relative density, mean and standard deviation of (U, V, W) and eventually [Fe/H] of each component to be compared to the model inputs. It is also possible to examine the ratios and orientation of principal axis of the velocity ellipsoid of each component but large error bars were obtained on these parameters which are not considered in this section. We have obtained 48 solutions with the simulated data (2 bins of distance, 2 models, 3 simulations per model, 3D and 4D deconvolution, 2 or 3 components assumed as initial condition). The deconvolution into 3 components was successful in very few cases, with a solution not physically realistic, one component having a very low standard deviation. Therefore we have only considered the deconvolutions into 2 components, all successful and stable. The corresponding averaged parameters are presented in Table 4, with their standard deviation. As expected, kinematical parameters and mean metallicities obtained for the thin disk in the 2 bins of distance are in the range of the Besançon model inputs (Table 3). However the relative density of the thin disk is found to be lower than expected in the first bin of distance. According to the density laws of the thin and thick disks adopted as inputs for the model, 87% of pseudostars should belong to the thin disk at 400 pc from the plane. On the other hand, we obtain a large error bar on this parameter, and the value of 78 ± 10% agrees within 1σ with the input of the model.

The error bars obtained for the thick disk are quite large and illustrate the difficulty to deconvolve overlapping populations.

The parameters of the deconvolved thick disk generally agree within 1σ with the model parameters in Table 3. For several parameters the agreement is within 2σ. We conclude that SEM is able to recover the mean parameters of the thin disk and the thick disk, even if they strongly overlap as in model 2, using 3D or 4D small samples ($N < 200$) affected by observational errors.

4.3.3. The thin and thick disks in the NGP sample

After these tests on simulated data, SEM was applied to the NGP sample. Each bin of distance includes 166 stars. We had to remove from the second bin, 2 outlier stars previously mentionned in Sect. 3.3. Results are presented in Table 5 in the 4D and 3D cases.

The success of the deconvolution of the sample into 2 discrete components supports the notion of a thick disk as a separate population, by opposition to being the tail of a continuous disk. Together with the existence of vertical gradients, this is of importance to constrain models.

In the nearest bin of distance, all the kinematical parameters obtained with the 3D and 4D deconvolution agree within 1σ, showing that [Fe/H] is less discriminant than velocities to separate the disk populations. In the 400–800 pc bin, a significant difference is observed in V when [Fe/H] is used in the deconvolution. However, the agreement being still within 2σ, we adopt as the final parameters for the thin disk the average of the 4 solutions (Table 6). The velocity ellipsoid $(\sigma_U, \sigma_V, \sigma_W) = (39 \pm 2, 20 \pm 2, 20 \pm 1)\,\mathrm{km\,s^{-1}}$ is typical of the old thin disk population. In their study of local kinematics from Hipparcos data, Dehnen & Binney (1998) and Bianaymé (1999) have determined dispersions for the oldest thin disk stars in the range 34–38 $\mathrm{km\,s^{-1}}$ in U, 23–25 $\mathrm{km\,s^{-1}}$ in V, 17–21 $\mathrm{km\,s^{-1}}$ in W. From stars at larger distances, we obtain similar values, showing that no significant vertical gradient is present in velocity dispersions of the thin disk.

The proportion of thick disk stars is higher than expected in the 2 bins of distance. If an exponential law with scale height of 800 pc is able to modelise the vertical density of the thick disk, then a local relative density of 15% has to be adopted to reproduce our results. On another hand, due to the small size of the sample, the proportions of each component cannot be recovered with a high accuracy, as was also seen with the simulated data. According to the dispersion of the SEM solutions on real and simulated data, we estimate our error bar on local density to be 7%.

Chiba & Beers (2000) found in their metal-poor star sample a vertical gradient in the rotational velocity of the thick disk of $-30\,\mathrm{km\,s^{-1}\,kpc^{-1}}$ which is not observed in the NGP sample. We note however a higher σ_W and lower [Fe/H] at 400–800 pc possibly indicating a vertical gradient. As the metallicity found for the thick disk (-0.27 and -0.42) is more metal-rich than expected, we have examined the eventuality of a bias in metallicity in our data. This high metallicity is mainly due to the lack of stars with [Fe/H] < -0.65. As discussed in Sect. 3.2.4, our method to estimate metallicities cannot explain by its own the complete absence of metal-poor stars. The selection of the target stars in the colour range $0.90 < B-V < 1.10$ may have also led to a lack of metal-poor stars. We have investigated the effect of this colour cut on metallicity on data simulated with the Besançon model and on giants of the TGMET library. If it is clear that deficient giants ([Fe/H] < -1.0) are bluer, the effect is not so dramatic in the range $-0.65 <$ [Fe/H] < -1.0. Selecting stars with $0.90 < B-V$ seems to eliminate about 30% of giants in this metallicity interval. Again, the lack of metal-poor stars cannot be completely explained by our colour cut. Besides, when testing the SEM algorithm on simulated data (Sect. 4.3.2), correct mean metallicities were recovered, despite a similar colour cut. *If this lack of low metallicities is real, an explanation would be that the missing metal-poor stars belong to another population with a higher scale height and lower local density*. However this hypothesis does not explain the high metallicity, [Fe/H] $= -0.27$, found for the thick disk in the nearest bin of distance. We interpret this value by the existence of stars with slow rotation but solar metallicity (Fig. 4). A population of metal-rich stars with thick disk kinematics is known to exist in the solar neighbourhood (Grenon 1999; Soubiran 1999). This population is found to have a flat distribution in the local disk and its origin near the bulge, with an orbital diffusion by a bar, is proposed (Martinet & Raboud 1999). These stars, which do not share the thick disk history, can also explain the lower $\sigma_W = 28 \pm 3\,\mathrm{km\,s^{-1}}$ found for the thick disk in the nearest bin of distance, instead of $\sigma_W = 39 \pm 4\,\mathrm{km\,s^{-1}}$ farther from the plane. These considerations led us to adopt as the best parameters for the thick disk the average of the 4D and 3D SEM solutions obtained in the bin 400–800 pc. The mean metallicity of -0.42 is probably still overestimated but yet favours the idea of a metal-rich thick disk. Our estimate of the mean metallicity of this population is [Fe/H] $= -0.48 \pm 0.05$. The adopted parameters of the thick disk are given in Table 6. As mentionned previously, numerous determinations of the kinematical parameters of the thick disk exist in the literature and span a wide range of values. Our determination is also in this range, but on the cooler side with moderate dispersions in V and W, and moderate asymmetric drift. On the contrary, $\sigma_U = 63 \pm 6\,\mathrm{km\,s^{-1}}$ is significantly higher than most of previous determinations which are often below $50\,\mathrm{km\,s^{-1}}$ (e.g. Morrison et al. 1990; Soubiran 1993; Chen 1997; Chiba & Beers 2000).

We conclude that our results favour a dense, flat, metal-rich thick disk with moderate rotational and vertical kinematics, but significant dispersion in radial motions. Our thick disk parameters fit nicely those found by Bell (1996) which also rely on a spectroscopic survey of 570 K giants, but in the rotation and antirotation directions. Similarly to us, he finds a lack of stars with [Fe/H] < -0.60. His sample is better described by a two-component disk model than by a continuous disk. He determines for the thick disk a mean abundance of -0.35 ± 0.06, an asymmetric drift of $-43 \pm 9\,\mathrm{km\,s^{-1}}$, and a local normalization of $13 \pm 3\%$. In terms of formation of the thick disk, the discreteness and absence of a vertical gradient suggest a quick heating of a precursor thin disk. This has to be replaced in a context where a merger is at present the prefered model for the origin of a thick disk in our galaxy and in other galaxies. The moderate parameters that we have determined favour the interpretation that we have observed in the NGP sample the puffed

Table 4. SEM deconvolution on the simulated data. The mean parameters are given with their standard deviation.

	%	[Fe/H]	$\sigma_{[Fe/H]}$	V_{lag} km s^{-1}	σ_U km s^{-1}	σ_V km s^{-1}	σ_W km s^{-1}
thin disk 200–400 pc	78 ± 10	−0.16 ± 0.08	0.23 ± 0.03	−16 ± 2	37 ± 4	24 ± 3	17 ± 4
thin disk 400–800 pc	75 ± 6	−0.17 ± 0.05	0.29 ± 0.02	−15 ± 6	40 ± 4	26 ± 3	16 ± 2
thick disk model 1 200–400 pc	21 ± 8	−0.58 ± 0.02	0.27 ± 0.02	−70 ± 10	78 ± 14	59 ± 5	41 ± 7
thick disk model 1 400–800 pc	24 ± 5	−0.71 ± 0.03	0.32 ± 0.02	−97 ± 3	73 ± 6	73 ± 11	50 ± 4
thick disk model 2 200–400 pc	19 ± 7	−0.50 ± 0.10	0.30 ± 0.05	−67 ± 9	56 ± 11	44 ± 7	29 ± 3
thick disk model 2 400–800 pc	31 ± 3	−0.42 ± 0.07	0.33 ± 0.01	−65 ± 11	70 ± 7	43 ± 7	35 ± 7

Table 5. 4D and 3D SEM deconvolution into 2 Gaussian components for the observed NGP sample, in 2 bins of distance. The parameters are given with their standard errors.

	%	[Fe/H]	$\sigma_{[Fe/H]}$	V_{lag} km s^{-1}	σ_U km s^{-1}	σ_V km s^{-1}	σ_W km s^{-1}
thin disk 200–400 pc 3D	77 ± 7	–	–	−11 ± 2	37 ± 2	17 ± 1	20 ± 1
thin disk 200–400 pc 4D	75 ± 7	−0.16 ± 0.01	0.23 ± 0.03	−11 ± 2	36 ± 2	17 ± 1	19 ± 1
thin disk 400–800 pc 3D	60 ± 6	–	–	−8 ± 3	39 ± 3	19 ± 1	23 ± 2
thin disk 400–800 pc 4D	65 ± 6	−0.19 ± 0.01	0.29 ± 0.02	−20 ± 3	44 ± 3	28 ± 2	19 ± 1
thick disk 200–400 pc 3D	23 ± 4	–	–	−69 ± 5	68 ± 8	33 ± 4	28 ± 3
thick disk 200–400 pc 4D	25 ± 4	−0.27 ± 0.03	0.27 ± 0.02	−65 ± 5	67 ± 7	34 ± 4	28 ± 3
thick disk 400–800 pc 3D	41 ± 5	–	–	−59 ± 4	64 ± 6	34 ± 3	36 ± 3
thick disk 400–800 pc 4D	35 ± 5	−0.42 ± 0.01	0.32 ± 0.02	−44 ± 6	62 ± 6	44 ± 4	42 ± 4

Table 6. Adopted parameters for the thin and thick disks from the deconvolution of the NGP sample. The relative densities are given for $z = 0$. The error bars were estimated from the dispersion of the SEM solutions on real and simulated data.

	%	[Fe/H]	$\sigma_{[Fe/H]}$	V_{lag} km s^{-1}	σ_U km s^{-1}	σ_V km s^{-1}	σ_W km s^{-1}
thin disk	85 ± 7	−0.17 ± 0.03	0.26 ± 0.03	−12 ± 2	39 ± 2	20 ± 2	20 ± 1
thick disk	15 ± 7	−0.48 ± 0.05	0.32 ± 0.03	−51 ± 5	63 ± 6	39 ± 4	39 ± 4

up early thin disk, whereas Gilmore et al. (2002) and Chiba & Beers (2000) have observed the relics of the disrupted satellite in the form of slower rotating metal-poor population. The existence of two components for the thick disk may reconcile the current inconsistent determinations of its scale height and normalisation.

5. Vertex deviation

The orientation of the velocity ellipsoid is of importance to test the axisymmetry and stationarity of the Galaxy. The vertex deviation, i.e. the inclination of the principal axis with respect to the direction of the Galactic Center is able to reveal distortions in the disk as described in Kuijken & Tremaine (1991). In order to follow the shape of the velocity ellipsoid with distance to the plane, the NGP sample was combined to a local sample constructed out of the Hipparcos catalogue. Its construction is described in Paper II. Briefly, this sample consists of mainly red clump giants, complete up to 125 pc, and corrected from the Lutz-Kelker bias. Radial velocities and metallicities were retrieved from the literature: 526 stars have radial velocities, 192 stars have metallicities from the literature and 111 have metallicities derived from Strömgren photometry. The NGP and local samples have been used to study the variations of the velocity ellipsoid with respect to [Fe/H] and distance to the plane, and were divided into 6 subsamples: [Fe/H] < -0.25, [Fe/H] > -0.25 and $z \leq 125$ pc, $200 < z < 400$ pc, $z > 400$ pc. The vertex deviation is determined by a linear fit in (U, V) for each subsample. Results are presented in Table 7 and Fig. 6.

Table 7. For each subsample, orientation in degree of the velocity ellipsoid from a linear regression on the (U, V) distribution. Errors range from 3° to 5°.

Selection	[Fe/H] < -0.25	[Fe/H] > -0.25
$z \geq 400$ pc	−1.7°	5.6°
200 pc $< z \leq 400$ pc	5.6°	13.3°
$z \leq 125$ pc	0.3°	16.4°

A positive vertex deviation (Fig. 6) is seen in the high metallicity sample in the 3 bins of distance, with however a smaller deviation in the highest bin. Kinematical groups are visible in the nearest bin of metal rich stars, suggesting a younger, partially mixed population. If we consider the inclination of the inner part of the ellipsoids, the vertex deviation is found to range between ∼13° and ∼25°. On the contrary, the low metallicity sample, dominated by thick disk stars, has a vertex deviation near zero. We may also remark that metal rich stars have velocity dispersions and vertex deviation intermediate between old disk and and thick disk in the highest bin.

It is well established and recently confirmed from Hipparcos data (Dehnen & Binney 1998; Bienaymé 1999) that

the vertex deviation declines from 25° for young stellar populations to near zero for older and kinematically hotter disk populations. This deviation of the vertex orientation has been frequently discussed (Kuijken & Tremaine 1994; Dehnen & Binney 1998; Binney & Merrifield 1998) and may imply either a non-axisymmetric Galaxy or local spiral perturbations or more simply partially mixed populations. Since the vertex deviation is not constant, the decline suggests that the deviation is caused by a small scale peturbation like a nearby spiral arm or by non-stationarity, the deviation reflecting the recent condition of formation of young stars. From Hipparcos data, Bienaymé (1999) finds that the vertex deviation is compatible with zero ($5 \pm 5°$) for the reddest Hipparcos stars (B-$V \sim 0.5$–0.7), while Dehnen & Binney (1998) obtain a $10 \pm 5°$ deviation for the same stars. From their respective result, they draw opposite conclusions concerning the axisymmetry or non-axisymmetry of the galactic disk, but we may remark that their measurements agree within 1σ error.

Here we find that the metallicity allows a more drastic separation of populations, and that the oldest and well-mixed population has a null vertex deviation. $B-V$ colours do not allow to separate very efficiently Hipparcos populations by age and the red Hipparcos stars are a mixture of old and a small proportion of young stars producing a non strictly null vertex deviation. This is clearly established, here, with the Hipparcos sample of giants with known metallicities.

In conclusion the vertex orientation of the oldest stars points towards the galactic center, favouring the hypothesis of an axisymmetric galactic disk (however if the galactic disk is elliptic and the Sun is located on one of the symetry axis, the vertex will also point towards the Galactic Center).

6. Conclusion

We have presented a new sample of nearly 400 stars selected out of the Tycho–2 catalog and observed at high spectral resolution. This sample mainly consists of red clump giants. Their atmospheric parameters ($T_{\rm eff}$, $\log g$, [Fe/H]) and absolute magnitudes M_v were estimated with the TGMET software by comparison to a reference library of spectra. The sample was used to investigate the kinematics and metallicity of the stellar disk up to 800 pc from the galactic plane with a typical error of 18% on distances, $3\,{\rm km\,s^{-1}}$ in U and V velocities, and lower than $1\,{\rm km\,s^{-1}}$ in W, at the mean distance of the sample (400 pc).

Our colour-magnitude cuts were efficient to select K giants since less than 6% of the sample consists in dwarfs or subgiants. We have observed in the sample a lack of metal-poor stars ([Fe/H] < -0.65) which is only partially explained by the method used to estimate the metallicities and by the colour cut. Velocity and metallicity distributions were compared to simulations of the Besançon model using 2 models of thick disk: a metal-poor kinematically hot one and another one with parameters closer to the thin disk. The NGP sample is in a better agreement with the moderate thick disk model. Using a non-informative method in the case of a mixture of Gaussian populations, we find our sample to be consistent with a superposition of two disks. The first one, associated the thin disk, has $V_{\rm lag} = -12 \pm 2\,{\rm km\,s^{-1}}$ with respect to the Sun, $(\sigma_U, \sigma_V, \sigma_W) = (39 \pm 2, 20 \pm 2, 20 \pm 1)\,{\rm km\,s^{-1}}$, [Fe/H] $= -0.17 \pm 0.01$, in agreement with previous studies from local samples. No vertical gradient is observed in the parameters of the thin disk.

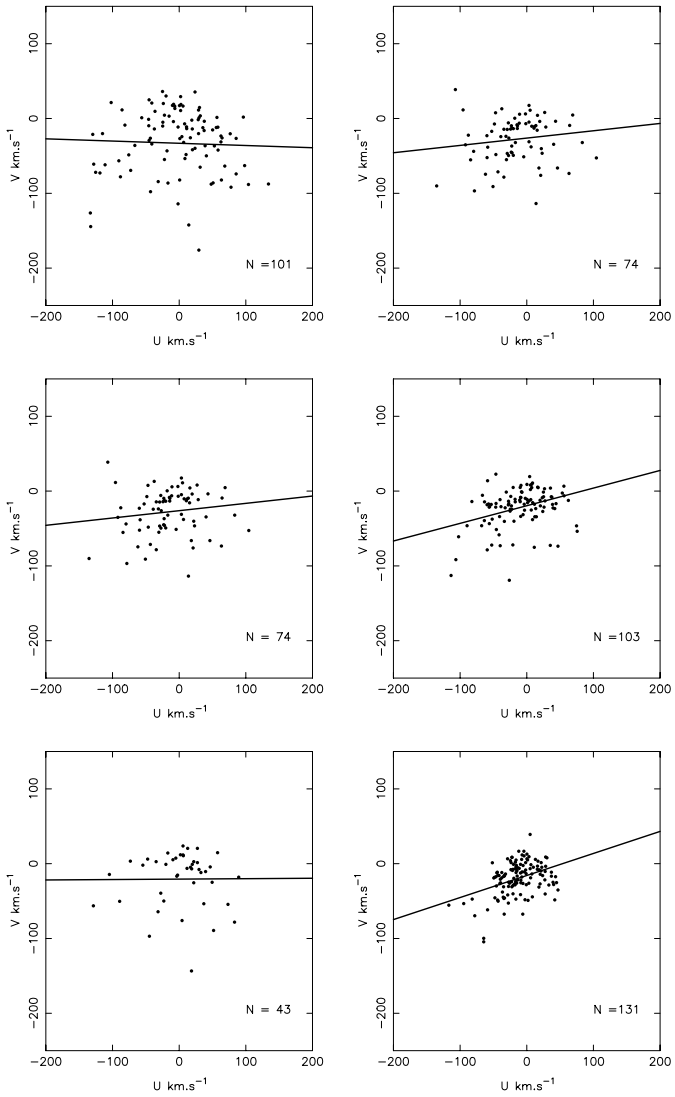

Fig. 6. (U, V) velocity distributions and vertex deviation. *Left:* selection with [Fe/H] < -0.25. *Right:* selection with [Fe/H] > -0.25. *From bottom to top:* $z < 125$ pc, 200 pc $< z <$ 400 pc, $z > 400$ pc.

The parameters of the thick disk were estimated to be $V_{\rm lag} = -51 \pm 5\,{\rm km\,s^{-1}}$, $(\sigma_U, \sigma_V, \sigma_W) = (63 \pm 6, 39 \pm 4, 39 \pm 4)\,{\rm km\,s^{-1}}$, [Fe/H] $= -0.48 \pm 0.05$. Compared to previous studies, these values are on the hot side for U, but on the cold, metal-rich side for V, W and [Fe/H]. The proportion of thick disk stars is found to be higher than expected with a local normalisation of $15 \pm 7\%$. Inconsistent determinations of the thick disk parameters in the recent literature may be reconcilied if 2 components are involved. In the context of the formation of the thick disc by a significant merger, we may have observed in the NGP sample the early heated thin disk, whereas other authors may have observed the relics of a shredded satellite.

The vertex deviation of the velocity ellipsoid has been studied with respect to distance above the plane and metallicity. For this task, the NGP sample was completed by a local Hipparcos

sample for which metallicity and radial velocities were retrieved from the literature. A null vertex deviation is found for the low metallicity subsample whereas the high metallicity sample exhibit a positive one. This suggests no strong deviation from axisymmetry of the galactic disk at solar radius.

The next paper of this series will give a new derivation of the mass density in the galactic plane based on these observations combined to the local Hipparcos sample. The sample presented in this paper, together with its Hipparcos counterpart, provides a sample with unprecedented accuracy to study the vertical potential up to 800 pc.

Acknowledgements. This research has made use of the SIMBAD and VIZIER databases, operated at CDS, Strasbourg, France. It is based on data from the ESA *Hipparcos* satellite (Hipparcos and Tycho–2 catalogues). We thank A. Robin who provided simulated samples from of new version of the Besançon model before publication.

References

Alonso, A., Arribas, S., & Martínez-Roger, C. 1999a, A&AS, 139, 335
Alonso, A., Arribas, S., & Martínez-Roger, C. 1999b, A&AS, 140, 261
Alonso, A., Arribas, S., & Martinez-Roger, C. 1996a, A&AS, 117, 227
Alonso, A., Arribas, S., & Martinez-Roger, C. 1996b, A&A, 313, 873
Baranne, A., Queloz, D., Mayor, M., et al. 1996, A&AS, 119, 373
Bell, D. C. 1996, Ph.D. Thesis, Univ. of Illinois
Bienaymé, O. 1999, A&A, 341, 86
Binney, J., & Merrifield, M. 1998, Galactic astronomy (Princeton, NJ: Princeton University Press), 1998
Blackwell, D. E., & Lynas-Gray, A. E. 1998, A&AS, 129, 505
Cayrel de Strobel, G., Soubiran, C., & Ralite, N. 2001, A&A, 373, 159
Celeux, G., & Diebolt, J. 1986, Rev. Stat. Appl., 35, 36
Chen, B. 1997, ApJ, 491, 181
Chiba, M., & Beers, T. C. 2000, AJ, 119, 2843
Crézé, M., Chereul, E., Bienaymé, O., & Pichon, C. 1998a, A&A, 329, 920
Crézé, M., Chereul, E., Bienaymé, O., & Pichon, C. 1998b, Proc. of the ESA Symp. Hipparcos - Venice 97, ESA SP-402, 669
Dehnen, W. 2000, AJ, 119, 800
Dehnen, W., & Binney, J. J. 1998, MNRAS, 298, 387
di Benedetto, G. P. 1998, A&A, 339, 858
ESA. 1997, The HIPPARCOS and TYCHO catalogues (Noordwijk, Netherlands: ESA Publications Division)
Flynn, C., & Freeman, K. C. 1993, A&AS, 97, 835
Gilmore, G., Wyse, R. F. G., & Norris, J. E. 2002, ApJL, 574
Girardi, L., & Salaris, M. 2001, MNRAS, 323, 109
Grenon, M. 1999, Ap&SS, 265, 331
Høg, E., Fabricius, C., Makarov, V. V., et al. 2000, A&A, 355, L27
Holmberg, J., & Flynn, C. 2000, MNRAS, 313, 209
Johnson, D. R. H., & Soderblom, D. R. 1987, AJ, 93, 864
Katz, D., Soubiran, C., Cayrel, R., Adda, M., & Cautain, R. 1998, A&A, 338, 151
Kuijken K., & Gilmore G. 1989, MNRAS, 239, 605
Kuijken, K., & Tremaine, S. 1991, in Dynamics of disc galaxies, Varberg Castle, Sweden, 71
Kuijken, K., & Tremaine, S. 1994, ApJ, 421, 178
Majewski, S. R. 1993, ARA&A, 31, 575
Martinet, L., & Raboud, D. 1999, Ap&SS, 265, 371
Morrison, H. L., Flynn, C., Freeman, K. C. 1990, AJ, 100, 1191
Morel, M., & Magnenat, P. 1978, A&AS, 34, 477
Norris, J. E. 1999, Ap&SS, 265, 213
Ojha, D. K., Bienaymé, O., Robin, A. C., Crézé, M., & Mohan, V. 1996, A&A, 311, 456
Paczynski, B. 1998, Acta Astron., 48, 405
Pham, H.-A. 1998, Proc. of the ESA Symp. Hipparcos - Venice 97, ESA SP-402, 559
Prugniel, P., & Soubiran, C. 2001, A&A, 369, 1048
Ratnatunga, K. U., & Freeman, K. C. 1989, ApJ, 339, 126
Reid, N., & Majewski, S. R. 1993, ApJ, 409, 635
Reylé, C., & Robin, A. C. 2001, A&A, 373, 886
Robin, A., & Crézé, M. 1986, A&A, 157, 71
Robin, A. C., Reylé, C., Derrière, S., & Picaud, S. 2002, A&A, submitted
Siebert, A., Bienaymé, O., & Soubiran, C. 2003, A&A, in press
Soubiran, C. 1993, A&A, 274, 181
Soubiran, C. 1999, Ap&SS, 265, 353
Soubiran, C., Katz, D., & Cayrel, R. 1998, A&AS, 133, 221